Effect of charge ordering/disordering on Raman line shape in manganites

S. Dattagupta*,‡
S. N. Bose National Centre for Basic Sciences, Block JD, Sector III, Salt Lake, Calcutta - 700091, India

A. K. Sood†,‡
Department of Physics, Indian Institute of Science, Bangalore - 560012, India

(Received 9 July 2001; revised manuscript received 5 September 2001; published 8 January 2002)

Manganites are characterized by a fascinating interplay of double exchange, spin and charge fluctuations, and orbital excitations. In this paper we focus attention on charge fluctuations and concomitant charge ordering/disordering, influenced by phonons. Our theoretical results, based on a resolvent expansion of the time-development operator (propagator), are specially tailored for calculating normal mode correlation functions, relevant for optic modes and the associated Raman scattering. The computed line shape, and the resultant line shift and linewidth, are compared with experiments in $Pr_{0.63}Ca_{0.37}MnO_3$. While the line shift data agree well with theory, the linewidth results indicate that charge (dis)ordering may not be the only relaxation mechanism in this system.

DOI: 10.1103/PhysRevB.65.064405 PACS number(s): 75.50.−y, 75.30.Vn, 75.70.Pa, 71.38.−k

I. INTRODUCTION

Manganites are systems of great interest in contemporary condensed matter physics. They exhibit a remarkable range of phenomena including metal-insulator transition, colossal and giant magnetoresistance, electron correlations, and charge/orbital ordering. We focus our discussion in the present work on charge ordering, especially in relation to Raman Scattering experiments.

Among the manganites the $3d$ transition metal oxides are characterized by relatively smaller bandwidths. Consequently, Coulomb correlation between charge carriers plays a dominant role in determining magnetic and electronic properties. One manifestation of this correlation is the occurrence of charge/orbital ordering. Examples of such systems are Fe_3O_4,[1] $La_{1-x}Sr_xNiO_4$ $(x=1/3,\frac{1}{2})$,[2] $La_{1-x}Sr_xFeO_3$ $(x=2/3)$,[3,4] $(La_{1-y}Nd_y)_{2-x}Sr_xCaO_4$ $(x=1/8)$,[5] and so on.

Perovskite-type manganese oxides, formulated as $RE_{1-x}AE_xMnO_3$, where RE and AE are a trivalent rare earth and an alkaline rare earth, are other prominent systems marked by an interplay of spin, charge, and orbital (lattice) degrees of freedom. For instance, in $REMnO_3$ (x=0) the electron configuration ($3d^4$; t_{2g}^3 e_g^1) is realized for the Mn^{3+} site, and due to ordering of the e_g orbital the substance is a layered antiferromagnetic insulator. In $RE_{1-x}AE_xMnO_3$, the substitution of RE^{3+} with AE^{2+} at the perovskite A site controls the mean Mn valence and a charge/orbital ordering, namely a real space ordering of Mn^{3+}/Mn^{4+} accompanied by a simultaneous ordering of e_g orbital of Mn^{3+}, is known to occur at $x\approx\frac{1}{2}$.

In this paper we present a fully dynamical theory of charge ordering, in which the dynamics is occasioned by the hopping of a charge from one site to a nearest neighbor site, in an underlying lattice gas model. In addition, we treat relaxational dynamics, caused by the coupling between the (charge) order parameter and phonons. It is the combination of these two kinds of dynamics which is envisaged to contribute to the broadening and shift of the Raman line shape. There will of course be a static line shift due to the presence of charge ordering itself.

With the preceding survey the outline and purpose of the present paper are as follows. In Sec. II A we present the Hamiltonian which forms the basis of all our calculations. This Hamiltonian describes charge ordering and hopping in a lattice gas picture besides, also, charge-phonon interaction. In Sec. II B we set up the calculational scheme for the Raman line shape. Section II C then contains a discussion of a unitary transformation on our basic Hamiltonian, which provides a convenient method of calculation. The complete line shape calculation is next presented in Sec. III. From the ''motional narrowing'' limit of the line shape, the line width and the line shift are extracted in Sec. III C. Because the starting point of our analysis is an *ab initio* Hamiltonian, the temperature dependence of the line shape parameters can be extracted from first principles. This calculation, involving one-phonon and two-phonon processes, is presented in Sec. III D. While the method of calculation and the derived results for the Raman line shape are of general validity for charge-ordered perovskites, we make specific comparison with the recently obtained Raman data in $Pr_{0.63}Ca_{0.37}MnO_3$.[6] This system, which is a paramagnetic insulator at room temperature, is characterized by an increase in resistivity as the temperature is lowered and a peak in magnetization at the charge ordering (CO) temperature $T_{CO}\approx 240$ K. However, the antiferromagnetic spin-ordering occurs not concurrently but at a lower temperature $T_N\approx 170$ K, and no ferromagnetic state is known to occur in zero field. The antiferromagnetic ordering is of the CE structure below T_{CO}, as has been confirmed by neutron diffraction study.[7] The temperature dependence of the two Raman active modes $A_g(2)$ and $A_g(4)$ shows that the peak position increases by about 10 cm^{-1} as the temperature is lowered from 300 K to 25 K.[6] This is much higher than what can be attributed to quasiharmonic or anharmonic contributions. Most interestingly, the temperature dependence of the linewidth is anomalous in that it increases on decreasing the temperature. Section IV is devoted to a detailed comparison between our theoretical results and the Raman data in $Pr_{0.63}Ca_{0.37}MnO_3$.[6] Finally, in Sec. V, we

offer a few concluding remarks, both on the present work as well as future directions.

II. THEORETICAL FORMULATION

A. The Hamiltonian

Following Lee and Min,[8] we formulate charge ordering, i.e., alternate ordering of Mn^{3+} and Mn^{4+}, in terms of a lattice gas/Ising model. Thus the presence or absence of a charge/electron on a lattice site is represented by an Ising spin, pointing up or down, respectively. The fully charge-ordered state then corresponds to an antiferromagnetic ground state of the pseudospins. This ground state can be disturbed in two distinct ways in which fluctuations make their presence felt: (i) thermal effects; and (ii) tunneling/hopping of the charge/electron between two near neighbor lattice sites. Clearly, in this picture, the effect of the Pauli exclusion principle is ignored, except that the hopping of an electron to an already occupied site is excluded. Thus the spin Hamiltonian can be written as

$$\mathcal{H}=\sum_{ij} V_{ij} s_i^z s_j^z + t \sum_{\langle ij \rangle} (s_i^+ s_j^- + s_i^- s_j^+), \tag{2.1}$$

where V_{ij} (>0) denotes the strength of antiferromagnetic coupling between pseudo-spins s_i^z, assuming z-axis to be the direction in which sublattice ordering occurs, whereas t is the strength of hopping, the latter being described in terms of the ladder operators $s_i^{\pm}$. The angular brackets over i and j depict nearest neighbor sites.

To Eq. (2.1) we must add the effect of lattice distortion when the electron resides at the Mn^{3+} site in view of the fact that Mn^{3+} is a Jahn-Teller ion. Following again Lee and Min,[8] and writing the displacement field in terms of phonon creation and annihilation operators, the Hamiltonian in Eq. (2.1) can be expanded as

$$\mathcal{H}_{L-M}=\mathcal{H}_s+\sum_i s_i^z \sum_{\underline{k}} G_i(\underline{k})(b_{\underline{k}}^\dagger + b_{\underline{k}}) + \sum_{\underline{k}} w_o(\underline{k}) b_{\underline{k}}^\dagger b_{\underline{k}}, \tag{2.2}$$

where $\mathcal{H}_s$ is the spin Hamiltonian described by the two terms in Eq. (2.1), $G_i(\underline{k})$ is the strength of the distortion field at the ith site $\underline{R}_i$ due to the kth phonon mode:

$$G_i(\underline{k})=G(\underline{k})e^{i\underline{k}.\underline{R}_i}, \tag{2.3}$$

$b_{\underline{k}}^\dagger(b_{\underline{k}})$ is the phonon creation (annihilation) operator, and $w_0(\underline{k})$ is the ''free'' phonon frequency. Lee and Min have calculated the shift in the phonon frequency based on Eq. (2.2) but have ignored the hopping term t. For our work t is crucial as it critically governs the Raman line shape, in general, and the linewidth, in particular. Thus the Lee-Min result for the line shift will naturally be a by-product of our result.

B. The Raman line shape

The Raman line shape is given by[9]

$$I_q(w)=\frac{1}{2\pi}\int_{-\infty}^{\infty} dt \exp(-iwt)\langle Q_{\underline{q}}(0) Q_{-\underline{q}}(t)\rangle, \tag{2.4}$$

where Q_q is the operator associated with the vibrational coordinate for the qth Raman active optic mode and the angular brackets indicate statistical average. The time dependence of $Q_{-\underline{q}}$ is governed by the usual Heisenberg evolution. Alternatively,

$$I_q(w)=\frac{1}{\pi}\mathrm{Re}\int_{-\infty}^{\infty} dt \exp(-iwt) C_q(t)=\frac{1}{\pi}\mathrm{Re}\,\tilde{C}_q(z), \quad (z=iw+\delta), \tag{2.5}$$

where $\tilde{C}_q(z)$ is the Laplace transform of the correlation function:

$$C_q(t)=\langle Q_{\underline{q}}(0) Q_{-\underline{q}}(t)\rangle. \tag{2.6}$$

Recall that we are interested in Raman transitions between the occupation number levels corresponding to $n_q=0$ and $n_q=1$ only, and involving a frequency of the order of 258 cm^{-1} ($\approx$370 K). Thus all other transitions are thermally forbidden as the Boltzmann population of the higher excited levels ($n_q>1$) is exceedingly small, even at room temperature.

Hence, it makes sense to isolate the two levels involved in the transition, ignore the other levels and represent these two levels with the aid of Pauli matrices, σ_z, σ_x, etc. Further, the rest of the phonon modes may be viewed to provide a ''phonon background,'' only passively participating in the underlying relaxation processes through the charge-ordering operator s_i^z. Thus the full Hamiltonian, relevant for Raman scattering, can be written as

$$\mathcal{H}=\frac{1}{2}\left[w_q \sigma_z + \sum_i g_{iq} s_i^z \sigma_x \right] + \mathcal{H}_{L-M}, \tag{2.7}$$

where $\mathcal{H}_{L-M}$, though still given by Eq. (2.2), is to be read such as to presume that the $k=q$ term is excluded from the summation. Since the phonon background (bath) comprises of a continuum of modes this exclusion is expected to have no discernible effect on the nature of the bath. In this simplified picture the transition operator $Q_{\underline{q}}$ may be replaced by σ_x, thus

$$C_{\underline{q}}(t)=A_{\underline{q}}\langle \sigma_x(0)\sigma_x(t)\rangle, \tag{2.8}$$

where A_q is an arbitrary q-dependent prefactor that can be absorbed in the intensity (or dropped altogether), and

$$\sigma_x(t)=\exp(i\mathcal{H}t)\sigma_x(0)\exp(-i\mathcal{H}t). \tag{2.9}$$

The Hamiltonian $\mathcal{H}$ in Eq. (2.7) belongs to a (very) large Hilbert space comprising of the two level space of σ, N two level spaces of $\underline{s}$ (N being the number of lattice sites), de-

noted by $\{s\}$, and the $3n$-dimensional space of the phonons, represented by $\{p\}$ where n is the number of atoms per unit cell.

C. Unitary transformation

As is customary in polaron physics,[10] it is convenient to eliminate the linear coupling term, i.e., the second term on the right hand side of Eq. (2.2), through a unitary transformation:

$$S=\exp\left[\sum_i s_i^z \sum_{\underline{k}} \frac{G_i(k)}{w_o(\underline{k})}(b_{\underline{k}}^\dagger - b_{\underline{k}})\right]. \tag{2.10}$$

Under this transformation the Hamiltonian $\mathcal{H}_{L-M}$ transforms into:[11]

$$\begin{aligned}\tilde{\mathcal{H}}_{L-M} &= S\mathcal{H}_{L-M}S^{-1} \\ &= \sum_{ij} \overline{V}_{ij} s_i^z s_j^z + t\sum_{\langle ij\rangle} (B_i^- B_j^+ s_i^+ s_j^- + B_i^+ B_j^- s_i^- s_j^+) \\ &\quad + \sum_{\underline{k}} w_o(\underline{k}) b_{\underline{k}}^\dagger b_{\underline{k}},\end{aligned} \tag{2.11}$$

where

$$B_i^{\pm} = \exp\left[\mp \sum_{\underline{k}} \frac{G_i(k)}{w_o(\underline{k})}(b_{\underline{k}}^\dagger - b_{\underline{k}})\right], \tag{2.12}$$

and

$$\overline{V}_{ij} = V_{ij} - \sum_{\underline{k}} \frac{G_i(k)G_j^*(k)}{w_0(\underline{k})}. \tag{2.13}$$

The full Hamiltonian in Eq. (2.7) then becomes

$$\tilde{\mathcal{H}} = \frac{1}{2}\left[w_{\underline{q}}\sigma_z + \sum_i g_{i\underline{q}} s_i^z \sigma_x\right] + \tilde{\mathcal{H}}_{L-M}. \tag{2.14}$$

Note that the correlation function in Eq. (2.8), and hence the line shape, remain invariant under the transformation in Eq. (2.10).

We may remark in passing that if the hopping term t is zero, the case considered by Lee and Min, the system $\{s\}$ is decoupled from the system $\{p\}$ and the operator s_i^z is a constant of motion [cf. Eq. (2.11)]. Thus $\tilde{\mathcal{H}}_{L-M}$ drops out from the time evolution of $\sigma_x(t)$ [see Eq. (2.9)] and we have

$$\sigma_x(t) = \exp(i\mathcal{H}_0 t)\sigma_x(0)\exp(-i\mathcal{H}_0 t), \tag{2.15}$$

where

$$\mathcal{H}_0 = \frac{1}{2}\left[w_{\underline{q}}\sigma_z + \sum_i g_{i\underline{q}} s_i^z \sigma_x\right]. \tag{2.16}$$

Using the property of Pauli matrices[12] we can easily calculate $\sigma_x(t)$ in Eq. (2.15), substitute the result in Eq. (2.8), and finally evaluate the line shape function in Eq. (2.5). The result is

$$I_q(w) = \frac{1}{4\pi}\mathrm{Re}\left\langle\left[\frac{1}{\delta - i(w+\sqrt{w_{\underline{q}}^2 + a_{\underline{q}}^2})} + \frac{1}{\delta - i(w-\sqrt{w_{\underline{q}}^2 + a_{\underline{q}}^2})}\right]\right\rangle, \tag{2.17}$$

where

$$a_{\underline{q}} = \sum_i g_{i\underline{q}} s_i^z, \tag{2.18}$$

and the angular brackets now denote statistical average governed by the Ising term, viz., the first term on the right hand side of Eq. (2.11). Considering only the Stokes term and employing mean-field approximation the Raman line position is given by

$$\overline{w}_{\underline{q}} \approx \left[w_{\underline{q}}^2 + \sum_{ij} g_{i\underline{q}} g_{j\underline{q}} \langle s_i^z s_j^z\rangle\right]^{1/2}. \tag{2.19}$$

This result is somewhat different from the one derived by Lee and Min. In particular, for optical frequencies, the first term inside the square parenthesis is much larger than the second. Thus,

$$\overline{w}_{\underline{q}} \approx w_{\underline{q}}\left[1 + \frac{1}{2}\sum_{ij} \frac{g_{i\underline{q}} g_{j\underline{q}}}{w_{\underline{q}}^2}\langle s_i^z s_j^z\rangle\right]. \tag{2.20}$$

Hence the line shift is given by

$$\Delta w_{\underline{q}} = \overline{w}_{\underline{q}} - w_{\underline{q}} = \frac{1}{2}\sum_{ij} \frac{g_{i\underline{q}} g_{j\underline{q}}}{w_{\underline{q}}}\langle s_i^z s_j^z\rangle. \tag{2.21}$$

We shall return to this result later in the context of experiment.

III. LINE SHAPE CALCULATION

A. Preliminaries

Before we embark on a perturbation theory calculation involving the many body Hamiltonian Eq. (2.14) it is useful to discuss in physical terms the logical sequence of the various steps involved. The first step is to recognize that the first term in $\tilde{\mathcal{H}}$ [cf. Eq. (2.14)], which is primarily responsible for the occurrence of the ''bare'' Raman line centered around w_q, is not influenced by $\tilde{\mathcal{H}}_{L-M}$ but for the presence of the charge-ordering operator s_i^z. The latter fluctuates in time, if we think in terms of an interaction picture treatment of $\tilde{\mathcal{H}}_{L-M}$. Alternately, we could adopt a stochastic formulation[13,14] in which $\tilde{\mathcal{H}}$ is replaced by a fully time dependent Hamiltonian:

$$\tilde{\mathcal{H}}(t) = \frac{1}{2}\left[\sigma_z w_{\underline{q}} + \sigma_x \sum_i g_{i\underline{q}} s_i^z(t)\right], \tag{3.1}$$

where $s_i^z(t)$ is a suitably modeled stochastic process, simulating the effect of the heat bath in which the system is embedded. While we shall present such a stochastic model calculation in Appendix B and compare with our many body

formulation, the whole idea of the many body treatment is in fact to extract the time dependence of $s_i^z(t)$ from first principles.

At this stage it is instructive to assess what the influence of the second term in the right of Eq. (3.1) on the eigenstates of the first term is expected to be. As σ_x is purely off-diagonal in the representation in which σ_z is diagonal, the second term causes transitions between the Raman active levels. This would produce a shift, the static component of which is already estimated in Eq. (2.19), and a width proportional to the mean square fluctuation in $\sigma_i^z(t)$. As the latter is expected to become more and more rapid as one approaches the charge-ordering temperature $T_{\rm CO}$ from below, the width is expected to decrease as the temperature increases to $T_{\rm CO}$. This qualitative picture is indeed what is seen in experiments,[6] as discussed in detail in Sec. IV, and is akin to the familiar ''motional narrowing effect'' in nuclear magnetic resonance.[15] In order to translate the above picture into concrete mathematical expressions we shall now focus our attention to $\tilde{\mathcal{H}}_{L-M}$ and split it as

$$\tilde{\mathcal{H}}_{L-M}=\mathcal{H}_s+\mathcal{H}_I+\mathcal{H}_p, \tag{3.2}$$

where $\mathcal{H}_s$ is the pseudo-spin part:

$$\mathcal{H}_s=\sum_{ij}\ \overline{V}_{ij}s_i^z s_j^z, \tag{3.3}$$

$\mathcal{H}_p$ is the phonon part:

$$\mathcal{H}_p=\sum_{\underline{k}}\ w_0(\underline{k})b_{\underline{k}}^{\dagger}b_{\underline{k}}, \tag{3.4}$$

and $\mathcal{H}_I$ is the interaction between the two parts:

$$\mathcal{H}_I=t\sum_{\langle ij\rangle}\ (B_i^- B_j^+ s_i^+ s_j^- + B_i^+ B_j^- s_i^- s_j^+). \tag{3.5}$$

Recall that in the calculation of the correlation function $\tilde{C}_q(z)$ we do not have to worry about any *direct* effect on the transition operator σ_x of the phonon system; instead we are interested in extracting the phonon-averaged time-development operator. The Laplace transform of the time-development operator can be written as

$$\mathcal{U}(z)=(z-i\mathcal{L})^{-1}, \tag{3.6}$$

where $\mathcal{L}$ is the Liouville operator[9] associated with the total Hamiltonian $\mathcal{H}$ in Eq. (2.14). The phonon-averaged time-development operator is then given by

$$(\mathcal{U}(z))_{av}=\frac{1}{Z_p}\sum_{\underline{n}_k,\underline{n}_k'}\exp(-\beta E_{\underline{n}_k})(\underline{n}_k,\underline{n}_k|\tilde{\mathcal{U}}(z)|\underline{n}_k',\underline{n}_k'), \tag{3.7}$$

where $E_{\underline{n}_k}$ is the energy eigenvalue of $\mathcal{H}_p$ defined by

$$\mathcal{H}_p|\underline{n}_k\rangle=E_{\underline{n}_k}|\underline{n}_k\rangle, \tag{3.8}$$

and Z_p is the partition function for the phonon system. In second order perturbation theory the averaged time-development operator reduces to:[9]

$$(\tilde{\mathcal{U}}(z))_{av}=[z-i\mathcal{L}_0+\tilde{\Sigma}(z)]^{-1}, \tag{3.9}$$

where $\tilde{\Sigma}(z)$ is the so-called ''self-energy:''

$$\tilde{\Sigma}(z)=\left(\mathcal{L}_I\frac{1}{z-i(\mathcal{L}_p+\mathcal{L}_s)}\mathcal{L}_I\right)_{av}, \tag{3.10}$$

where different script $\mathcal{L}$'s represent Liouville operators associated with different parts of the Hamiltonian, denoted by the respective subscripts. It is pertinent to mention here that it is the Markovian limit of $\tilde{\Sigma}(z)$ (i.e., $z\to 0$) is what appears as the relaxation matrix in the stochastic model calcuation (see Appendix B).

B. Self-energy in mean field approximation

Recall that we are interested in the partially charge-ordered regime below $T_{\rm CO}$ (and above T_N) which exhibits antiferromagnetic ordering of the pseudo-spins. In mean-field theory the antiferromagnetic phase splits into two sublattices *A* and *B*, with alternate up and down spin orientations. Thus it makes sense to isolate *one* central spin, say 0 which, without loss of generality, can be assumed to belong to sublattice *A*. (Clearly, for a translationally invariant system, the results would be the same if the central spin were chosen to belong to sublattice *B*.) In this simplified picture the Hamiltonian $\tilde{\mathcal{H}}$ in Eq. (2.14) can be rewritten as

$$\tilde{\mathcal{H}}=\mathcal{H}_0+\mathcal{H}_s+\mathcal{H}_p+\mathcal{H}_I, \tag{3.11}$$

where, now

$$\mathcal{H}_0=\tfrac{1}{2}(w_{\underline{q}}\sigma_z+g_{\underline{q}}s_0^z\sigma_x), \tag{3.12}$$

$$\mathcal{H}_I=t\sum_l{}'\ (B_0^- B_l^+ s_0^+ s_l^- + B_0^+ B_l^- s_0^- s_l^+), \tag{3.13}$$

the prime indicating that the sum over *l* goes over the nearest neighbor sites of 0, which therefore belong to the sublattice *B*.

One other point merits attention. Since it is only the central spin s_0^z that participates directly in the Raman transitions, all other spins have to be lumped into what is regarded as the heat bath. Thus, the meaning of $(\ldots)_{av}$ in Eq. (3.7) has to be expanded in order to encompass not just the average over the phonon states but also the one over the eigenstates of all *other* spins, excluding the central spin. Therefore,

$$(\tilde{\mathcal{U}}(z))_{av}=\frac{1}{Z_pZ_s}\sum_{\underline{n}_k\underline{n}_k'}\sum_{ss'}\ e^{-\beta(E_{\underline{n}_k}+E_s)}\times(\underline{n}_k s,\underline{n}_k s|\tilde{\mathcal{U}}(z)|\underline{n}_k' s',\underline{n}_k' s'), \tag{3.14}$$

where E_s is the energy eigenvalue of the Ising spin Hamiltonian (excluding the central spin) and Z_s is the corresponding partition function. Needless to say, $\{s\}$ describes collec-

tively the spin configuration $\{s_1, s_2, \ldots\}$. Of course, $(U(z))_{av}$ is still given by Eq. (3.9), but now the self-energy is [cf. Eq. (3.10)]:

$$\tilde{\Sigma}(z) = \frac{1}{Z_p Z_s} \sum_{\underline{n}_k \underline{n}_k'} \sum_{ss'} e^{-\beta(E_{\underline{n}_k} + E_s)} \times \left(\underline{n}_k s, \underline{n}_k s \left| \left(\mathcal{L}_I \frac{1}{z - i(\mathcal{L}_p + \mathcal{L}_s)} \mathcal{L}_I \right) \right| \underline{n}_k' s', \underline{n}_k' s' \right). \tag{3.15}$$

It may be noted that $\tilde{\Sigma}(z)$ is a superoperator in the restricted Hilbert space of s_0^z alone as all other degrees of freedom are averaged over in Eq. (3.15). Since the operator σ_x involved in the Raman transition commutes with s_0^z, the specific matrix elements of $\tilde{\Sigma}(z)$ that are required in the line shape expression [cf. Eq. (2.8)] are of the type

$$\tilde{\Sigma}_{m_0, m_0'}(z) = (m_0, m_0 | \tilde{\Sigma}(z) | m_0', m_0'), \tag{3.16}$$

where the single site states $|m_0\rangle$ and $|m_0'\rangle$ are the eigenstates of s_0^z:

$$s_0^z |m_0\rangle = m_0 |m_0\rangle,$$

$$s_0^z |m_0'\rangle = m_0' |m_0'\rangle, \tag{3.17}$$

the allowed values of m_0 and m_0' being $\frac{1}{2}$ and $-\frac{1}{2}$. Thus there are only *four* relevant matrix elements of $\tilde{\Sigma}(z)$. These are computed in Appendix A, in the Markovian limit and are reproduced here:

$$(++|\tilde{\Sigma}(0)|++) = -(++|\tilde{\Sigma}(0)|--) = \lambda p_-, \tag{3.18}$$

and

$$(--|\tilde{\Sigma}(0)|--) = -(--|\tilde{\Sigma}(0)|++) = \lambda p_+, \tag{3.19}$$

where λ is the ''relaxation rate,'' given by

$$\lambda = \eta t^2 \int_{-\infty}^{\infty} d\tau \exp(-2iJ(0)M\tau) \xi(\tau), \tag{3.20}$$

$$\xi(\tau) = \exp\left\{ -\int dw \frac{j(w)}{w^2} \coth\left(\frac{1}{4}\beta w \right) \right\} \times \left[\exp \int dw \frac{j(w)}{w^2} \frac{\cos w\tau}{\sinh(\frac{1}{4}\beta w)} \right], \tag{3.21}$$

η being the number of nearest neighbor sites, M is the sublattice magnetization, $j(w)$ is the phonon density of states and $p_\pm$ are the Boltzmann populations for the states $|m_0\rangle = |\frac{1}{2}\rangle$ and $|m_0\rangle = |-\frac{1}{2}\rangle$, respectively. Since the mean-field Hamiltonian for the central spin, located in the A sublattice, is given by

$$\mathcal{H}_s^0 = J(0) M s_0^z,$$

$$J(0) = \sum_j \overline{V}_{ij}, \tag{3.22}$$

the occupation probabilities are:

$$p_\pm = \frac{e^{\mp \frac{1}{2} J(0) M\beta}}{e^{\frac{1}{2} J(0) M\beta} + e^{-\frac{1}{2} J(0) M\beta}}. \tag{3.23}$$

As is shown in Appendix B, expressions (3.18) and (3.19) are in conformity with detailed balance of transitions.

C. The line shape and its "motional narrowing" limit

At this stage it is pertinent to point out that the many body calculation based on the resolvent operator technique, presented above, yields an expression for the line shape which is identical to the one derived in the stochastic formulation, in the Markovian limit (see Appendix B). However, the advantage of the many body treatment is that within the same formalism one also obtains a calculable expression for the relaxation rate λ. This situation should be contrasted with the stochastic theory in which λ appears merely as a parameter.

With this background we refer back to Appendix B and note that

$$\tilde{\Sigma}(0) = \lambda(1 - \mathcal{J}), \tag{3.24}$$

where the transition matrix, which was introduced earlier in Appendix B, has the special structure

$$(m_0 m_0'' | \mathcal{J} | m_0' m_0''') = p_{m_0'} \delta_{m_0 m_0''} \delta_{m_0' m_0'''}. \tag{3.25}$$

Recall that in evaluating the angular brackets in Eq. (2.8), the superoperator $(\tilde{\mathcal{U}}(z))_{av}$ has to be further averaged over the states of the central spin s_0^z. Denoting this averaging by an overhead bar, we have

$$(\overline{\mathcal{U}(z)})_{av} = \sum_{m_0 m_0'} p_{m_0} \left(m_0, m_0 \left| \frac{1}{(z+\lambda) - i\mathcal{L}_0 - \lambda\mathcal{J}} \right| m_0', m_0' \right). \tag{3.26}$$

The structure of $\mathcal{J}$ as in Eq. (3.25) allows us to simplify the above expression as[9,14]

$$(\overline{\mathcal{U}(z)}) = [(\overline{\mathcal{U}^0(z+\lambda)})^{-1} - \lambda]^{-1}, \tag{3.27}$$

where

$$(\overline{\mathcal{U}^0(z+\lambda)}) = \sum_{m_0 m_0'} p_{m_0} \left(m_0, m_0 \left| \frac{1}{(z+\lambda) - i\mathcal{L}_0} \right| m_0', m_0' \right). \tag{3.28}$$

Note that $\mathcal{L}_0$ is the Liouville operator associated with the Hamiltonian $\mathcal{H}$ given by Eq. (3.12). In the regime of rapid relaxation it makes sense to further split $\mathcal{H}_0$ as

$$\mathcal{H}_0 = \overline{\mathcal{H}}_0 + V, \tag{3.29}$$

where

$$\overline{\mathcal{H}_0}=\frac{1}{2}w_{\underline{q}}\sigma_z, \tag{3.30}$$

and

$$V=\frac{1}{2}g_{\underline{q}}\sigma_x s_0^z, \tag{3.31}$$

and develop the coupling term, proportional to $g_{\underline{q}}$ as perturbation. Thus, denoting the corresponding Liouville operators as $\overline{\mathcal{L}_0}$ and $\mathcal{L}_v$, respectively, we may derive:[14]

$$(\overline{\mathcal{U}^0(z+\lambda)})^{-1}\cong(z+\lambda-i\overline{\mathcal{L}_0})-\frac{i}{2}g_{\underline{q}}M\sigma_x^{\times}+\sigma_x^{\times}\frac{\frac{1}{4}g_{\underline{q}}^2(1-M^2)}{z+\lambda-i\overline{\mathcal{L}_0}}\sigma_x^{\times}, \tag{3.32}$$

where the superscript cross denotes Liouville operators and M, the sublattice magnetization, is obtained from

$$M=\sum_{m_0}p_{m_0}m_0. \tag{3.33}$$

Therefore, from Eq. (3.27),

$$(\overline{\mathcal{U}(z)})_{av}=z-i\overline{\mathcal{L}_0}-\frac{i}{2}g_{\underline{q}}M\sigma_x^{\times}+\sigma_x^{\times}\frac{\frac{1}{4}g_{\underline{q}}^2(1-M^2)}{z+\lambda-i\overline{\mathcal{L}_0}}\sigma_x^{\times}. \tag{3.34}$$

The complete line shape is then given by [cf. Eq. (2.8)]

$$\tilde{C}_q(z)=\sum_{\substack{\mu\nu\\ \mu'\nu'}}\langle\mu|\sigma_x|\mu'\rangle\langle\nu'|\sigma_x|\nu\rangle(\mu'\mu|(\overline{\mathcal{U}(z)})_{av}|\nu'\nu), \tag{3.35}$$

where $|\mu\rangle$, $|\nu\rangle$, etc. are the eigenslates of σ_z. Thus

$$\tilde{C}_q(z)=(+-|\overline{\mathcal{U}^0(z)}|+-)+(-+|\overline{\mathcal{U}^0(z)}|-+)+(+-|\overline{\mathcal{U}^0(z)}|-+)+(-+|\overline{\mathcal{U}^0(z)}|+-). \tag{3.36}$$

A few limiting cases may now be discussed.

1. "Static" shift

If the hopping term t is neglected (the Lee-Min limit) the relaxation rate λ goes to zero and the Laplace transform of the averaged time-development operator in Eq. (3.26) reduces to the Laplace transform of the unperturbed time-development operator, i.e.,

$$(\overline{\mathcal{U}(z)})_{av}=\overline{\mathcal{U}^0(z)}=\frac{1}{z-i\overline{\mathcal{L}_0}+\frac{i}{2}g_{\underline{q}}M\sigma_x^{\times}}. \tag{3.37}$$

From the structure of $\overline{\mathcal{L}_0}$ [cf. Eq. (3.30)], it is evident that the characteristic frequency is now given by

$$\overline{w_{\underline{q}}}=(w_{\underline{q}}^2+g_{\underline{q}}^2M^2)^{1/2}. \tag{3.38}$$

This is the mean-field version of Eq. (2.19). Following our discussion after Eq. (2.19), the line shift, for optical frequencies, is given by

$$\Delta w_{\underline{q}}=\frac{1}{2}\frac{g_{\underline{q}}^2}{\overline{w_{\underline{q}}}}M^2. \tag{3.39}$$

2. "Dynamic" shift and width

The effect of relaxational dynamics, occasioned by the phonon-mediated hopping of charges, is encapsulated within the fourth term inside the curly brackets in Eq. (3.34). Since the effect of static shift has already been estimated above, we shall ignore the third term and write

$$(\overline{\mathcal{U}(z)})_{av}=\left\{z-i\overline{\mathcal{L}_0}+\tfrac{1}{4}g_{\underline{q}}^2(1-M^2)\sigma_x^{\times}\frac{1}{z+\lambda-i\overline{\mathcal{L}_0}}\sigma_x^{\times}\right\}^{-1}. \tag{3.40}$$

The 4×4 matrix inside the curly brackets in Eq. (3.40) can be written as (where the rows and columns are labeled by $++$, $--$, $+-$, and $-+$)

$$\begin{bmatrix} z+\frac{2\alpha\overline{z}}{\overline{z}^2+w_{\underline{q}}^2} & -\frac{2\alpha\overline{z}}{\overline{z}^2+w_{\underline{q}}^2} & 0 & 0\\ -\frac{2\alpha\overline{z}}{\overline{z}^2+w_{\underline{q}}^2} & z+\frac{2\alpha\overline{z}}{\overline{z}^2+w_{\underline{q}}^2} & 0 & 0\\ 0 & 0 & z-iw_{\underline{q}}+\frac{2\alpha}{\overline{z}} & -\frac{2\alpha}{\overline{z}}\\ 0 & 0 & -\frac{2\alpha}{\overline{z}} & z+iw_{\underline{q}}+\frac{2\alpha}{\overline{z}} \end{bmatrix}, \tag{3.41}$$

where

$$\alpha=\tfrac{1}{4}g_q^2(1-M^2),\qquad \overline{z}=z+\lambda. \tag{3.42}$$

It is clear from Eq. (3.36) that it is only the lower 2×2 block in Eq. (3.41) which is relevant for the line shape calculation. After inverting this block and summing all the four elements, as required by Eq. (3.36), we have

$$\tilde{C}_q(z)=\frac{2}{\left(z^2+w_{\underline{q}}^2+\frac{4\alpha z}{\overline{z}}\right)}\left(z+\frac{4\alpha}{\overline{z}}\right), \tag{3.43}$$

which can be further simplified, in the regime of rapid relaxation, as

$$\tilde{C}_q(z)=\frac{2}{\left(z+\frac{w_{\underline{q}}^2}{z+\frac{4\alpha}{\lambda}}\right)}. \tag{3.44}$$

Denoting

$$\Gamma=\frac{4\alpha}{\lambda}=\frac{g_{\underline{q}}^2(1-M^2)}{\lambda}, \tag{3.45}$$

Eq. (3.44) can be written as a sum of two terms:

$$\tilde{C}_q(z)=\frac{1-\frac{i\Gamma/2}{w_{\underline{q}}\sqrt{1-\Gamma^2/4w_{\underline{q}}^2}}}{z+\frac{\Gamma}{2}-iw_{\underline{q}}\sqrt{1-\Gamma^2/4w_{\underline{q}}^2}} + \frac{1+\frac{i\Gamma/2}{w_{\underline{q}}\sqrt{1-\Gamma^2/4w_{\underline{q}}^2}}}{z+\frac{\Gamma}{2}+iw_{\underline{q}}\sqrt{1-\Gamma^2/4w_{\underline{q}}^2}}. \tag{3.46}$$

Thus the ''dynamic'' width is given by Γ in Eq. (3.45) whereas the ''dynamic'' shift is $\Gamma^2/8w_q$. Combining with Eq. (3.39), the net line shift is given by

$$\Delta w_q=\frac{1}{2}\frac{g_{\underline{q}}^2}{w_{\underline{q}}}\left[M^2+\frac{1}{4}\left(\frac{g_{\underline{q}}}{\lambda}\right)^2(1-M^2)^2\right]. \tag{3.47}$$

D. Temperature dependence of the linewidth

As discussed above, the linewidth is given by Eq. (3.45). Thus there are two sources of the temperature dependence of Γ, one arising from the temperature dependence of the order parameter M:

$$M=\tanh\left(\frac{T_{\rm CO}}{T}M\right),$$

$$T_{\rm CO}=\frac{1}{2}\frac{J(0)}{K}, \tag{3.48}$$

and the other from that of the relaxation rate λ.

In order to extract the temperature dependence of λ, one has to evaluate the integral in Eq. (3.21). Such an integral is known to occur in various contexts of polarons,[10] radiationless transitions,[17] phonon-assisted tunneling of light intenstitials in metals,[16,18,19] etc. As is well known in the literature, the terms corresponding to one-, two-, etc. phonon processes are obtained by expanding the exponential in the square brackets in Eq. (3.21) in a power series. These processes contribute different temperature dependencies. Normally, one-phonon processes can be neglected and the two-phonon processes yield:[18]

$$\lambda_2(T)\propto T^7,$$

$$T\ll\Theta_D, \tag{3.49}$$

or

$$\propto\left(\frac{1}{E_aKT}\right)^{1/2}\exp\left(-\frac{E_a}{KT}\right),$$

$$T\gg\Theta_D, \tag{3.50}$$

where Θ_D is the Debye temperature and the activation energy E_a is the so-called ''coincidence energy.'' However, in an important paper by Teichler and Seeger,[19] it has been pointed out that one-phonon contributions are significant when the distortion fields at the two sites involved in the hopping process are distinct. Because this is indeed the case for charge hopping between Mn^{3+} and Mn^{4+} sites, Mn^{3+} being a Jahn-Teller ion, we must reckon with this particular effect, which yields

$$\lambda_1(T)\propto T,$$

$$T\ll\Theta_D. \tag{3.51}$$

For the system $Pr_{0.63}Ca_{0.37}MnO_3$ at hand, the Debye temperature is substantially larger than the charge-ordering temperature $T_{\rm CO}$. Hence, in order to fit the date we have considered

$$\Gamma(T)=g_{\underline{q}}^2\frac{(1-M^2)}{(T+aT^7)}. \tag{3.52}$$

where a is an arbitrary fitting parameter.

IV. COMPARISON WITH DATA IN $Pr_{0.63}Ca_{0.37}MnO_3$

In this section we turn our attention to the analysis of Raman scattering experiments, performed in single crystals of $Pr_{0.63}Ca_{0.37}MnO_3$, over a temperature range of 20 K–300 K. The studies reveal strong anomalous temperature dependence of line shift and line width of the two Raman active A_g modes. The details of the experiment, the symmetry analyses and the origin of the relevant optic modes have been communicated recently.[20] It turns out that only two modes, $A_g(2)$ centered on 258 cm^{-1} and involving in-phase rotation of the in-plane oxygen cage, and $A_g(4)$ centered on 289 cm^{-1} and involving out-of-phase rotation of the apical oxygen, are prominently observable, upto room temperature. We discuss below, section wise, how the data compare with the theoretical results presented in Sec. III.

A. The line shift

As we mentioned before, the line shift has been calculated earlier by Lee and Min, albeit in the context of ultrasonic measurements involving acoustic phonons. There are two distinct ways in which our result in Eq. (3.47) goes beyond that of Lee and Min. First, of course, is the presence of the second term in square parentheses in Eq. (3.47), which originates from the phonon bath-induced relaxation dynamics.

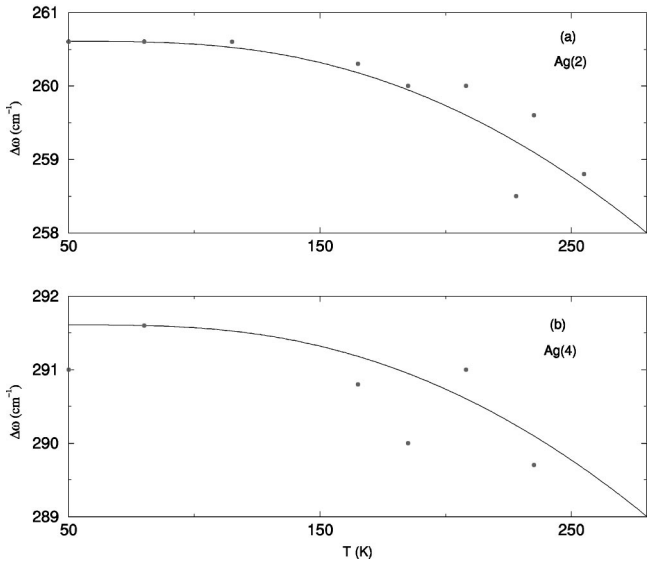

FIG. 1. The line shift (in cm^{-1}) based on Eq. (3.39), where M is given by Eq. (3.48) and T_{CO} has been fixed at 280 K, is plotted versus temperature from 50 K to 280 K: (a) For the mode frequency $w_q = 258\ cm^{-1}$. By equating the theoretical result ($=2.6\ cm^{-1}$) with the data point at $T=80$ K, the value of the coupling constant has been deduced as $g_q = 36.7\ cm^{-1}$; (b) for the mode frequency $w_q = 289\ cm^{-1}$. Again, by fixing the theory ($=2.6\ cm^{-1}$) with data point at $T=80$ K, we find $g_q = 38.8\ cm^{-1}$. The data points (Ref. 6) have been shown as solid circles.

This was not treated by Lee and Min. Apart from that, even when it comes to computing the static line shift, our result, given by the first term in Eq. (3.47), is different. This is because we have an explicit expression, derived in mean-field theory and for optical frequencies, relevant for Raman scattering.

It turns out, however, that the dynamical contribution to line shift, given by the second term in Eq. (3.47), is of order $(g_q/\lambda)^2$, and is therefore, negligibly small compared to the static shift. We have verified this point numerically. Therefore, what we have plotted in Fig. 1(a) and Fig. 1(b) is simply the contribution of the first term in Eq. (3.47), in which the order parameter M has been computed self-consistently from the mean-field solution (3.48).

A few comments are in order regarding the fitting of the data with theory. In the observed data there is a sharp change in the mode frequency at around 50 K, which has been attributed to the presence of a canted antiferromagnetic insulator phase below that temperature. Since the physics of this phase has not been included in our theory, the data analysis has been made only for temperatures above 50 K. Second, we have set the critical charge-ordering temperature T_{CO} at 280 K for the purpose of comparison with experiment, because mean-field theory is known to overestimate the transition temperature by at least about 10%. Finally, the only fitting parameter left is the coupling constant g_q. Since M saturates to unity below around 80 K and w_q for both the $A_g(2)$ and $A_g(4)$ modes are known we have evaluated g_q by equating the experimental data point at $T=80$ K to the theoretical value. The results are: $g_q = 36.7\ cm^{-1}$ for $A_g(2)$ mode and $g_q = 38.8\ cm^{-1}$ for $A_g(4)$ mode. Having thus determined g_q we employ these values in the rest of the fit as well as in the analysis of the linewidth data, given below.

In Fig. 1(a) we display the line shift result as a function of temperature, along with raw data, for the $A_g(2)$ mode: $w_q = 258\ cm^{-1}$, and fixed values for $g_q = 36.7\ cm^{-1}$ and $T_{CO} = 280$ K. Figure 1(b) exhibits similar plots, but now for the $A_g(4)$ mode: $289\ cm^{-1}$ and derived value of $g_q = 38.8\ cm^{-1}$, while the mean field transition temperature for charge ordering is kept fixed at 280 K. The agreement between theory and experiment seems quite satisfactory. One point is worth remarking here. Since M is nearly unity at 80 K at which temperature Δw_q is identical ($=2.6\ cm^{-1}$, from the digital data[6]), the ratio g_q^2/w_q is the same [$=5.2\ cm^{-1}$, cf. Eq. (3.39)] for both the $A_g(2)$ and $A_g(4)$ modes. Thus an important conclusion is that the line shift simply scales with the square of the order parameter.

B. The linewidth

Before we analyze the linewidth based on Eq. (3.52) we should point out that the narrowing of the Raman line in our treatment arises entirely from charge-disordering process, caused by intersite hopping of charges, triggered by phonons. Therefore, at temperatures much lower than T_{CO}, when charge ordering is complete, it is expected that hopping of charges would also be rare events, having a negligible influence on relaxational phenomena. This is clearly reflected in Eq. (3.52) which shows that the width goes to zero when the order parameter M saturates to unity.

From the discussion in the above paragraph it is evident that charge disordering cannot be the sole reason for the dynamic linewidth. It was mentioned earlier that the system at hand, $Pr_{0.63}Ca_{0.37}MnO_3$, is marked by an antiferromagnetic transition at a Neel temperature $T_N \approx 170$ K. Hence, it is expected that below T_N there would be significant (magnetic) spin fluctuation effects which might contribute to the Raman linewidth.

In a scenario, completely different from our charge (dis)ordering mechanism, Pai and Ramakrishnan have considered a spin-phonon interaction involving the t_{2g} spins and the A_g modes.[21] Using a Schwinger boson model for spin excitations and treating the spin-phonon coupling in second order perturbation theory, Pai and Ramakrishnan have calculated the decay rate for the A_g phonons. This could be a plausible mechanism for the observed linewidth at low temperatures and mode softening at temperatures of order T_N or somewhat higher.

We come back now to our linewidth result, originating from charge-(dis)ordering processes and plot in Fig. 2(a) the expression given by Eq. (3.52) for the $A_g(2)$ mode at $w_q = 258\ cm^{-1}$ for which we had estimated earlier from the line shift fit, the value $g_q = 36.7\ cm^{-1}$ for the coupling constant. A similar plot is given in Fig. 2(b), but now for the $A_g(4)$ mode at $w_q = 289\ cm^{-1}$ and $g_q = 38.8\ cm^{-1}$. In both Fig. 2(a) and Fig. 2(b), the value of the parameter a has been estimated to be around 10^{-14}. Although the value of a is so

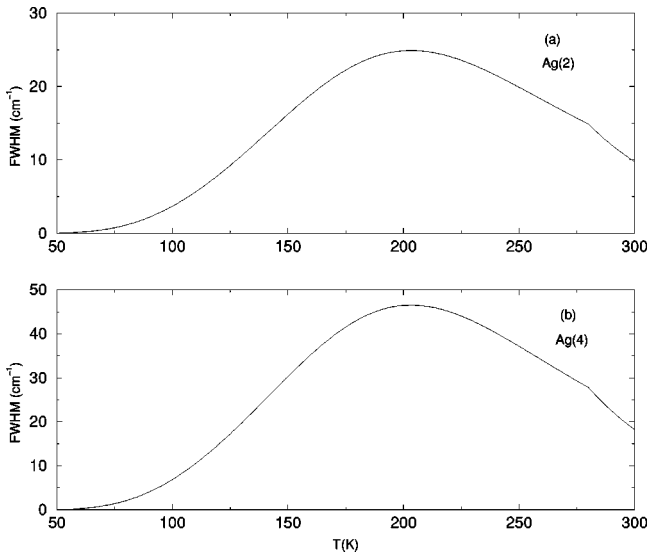

FIG. 2. The linewidth (in cm^{-1}) based on Eq. (3.52) has been plotted against temperature from 50 K to 300 K: (a) The coupling constant g_q has been fixed at what has been deduced for the $A_g(2)$ mode in Fig. 1(a). An overall scale factor 18 has been lumped as a prefactor in Eq. (3.52), arising from the strength of λ, whereas a has been estimated as 10^{-14}; (b) the value of the coupling constant now is $g_q = 38.8$ cm^{-1}, as in Fig. 1(b), and the prefactor in Eq. (3.52) has been taken as 30.

small, the two-phonon contribution (proportional to T^7) dominates over the one-phonon contribution (proportional to T), above 150 K!

For reasons mentioned before, we do not attach much credence to the linewidth result below 200 K, keeping in mind that the antiferromagnetic Neel temperature T_N is around 170 K, at least as far as the system $Pr_{0.63}Ca_{0.37}MnO_3$ is concerned. Therefore, we have replotted our theoretical results for the linewidth, along with raw data points,[6] in the temperature range of 200 K–300 K, both for the $A_g(2)$ and $A_g(4)$ modes, in Figs. 3(a) and 3(b), respectively. Considering that the coupling constants are *derived* from the line shift data and are no longer fitting parameters, and the only fitting parameter left is the relative weightage ''a'' of one-phonon versus two-phonon processes, the agreement between theory and experiment between 200 K and 300 K is remarkably good.

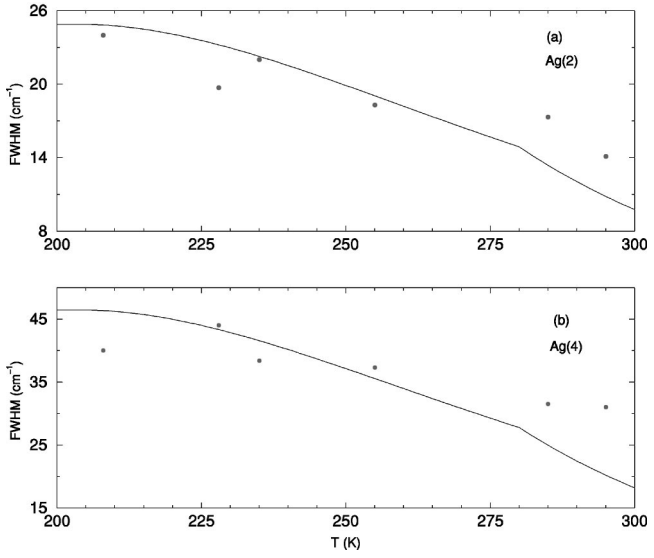

FIG. 3. The results in (a) Fig. 2(a) and 2(b) along with raw data points (Ref. 6) are replotted, but now in the temperature range 200 K to 300 K.

V. SUMMARY AND CONCLUSIONS

We have addressed in detail in this paper the issue of charge ordering which is considered to be ubiquitous in the topically important materials of manganites. The many body theory we have formulated has been specifically geared to carefully scrutinizing questions in the context of the Raman line shape. The resolvent operator technique, in conjunction with the mean-field approximation, has enabled us to derive expressions for the line shape, which can be compared and contrasted with explicit stochastic considerations.

The coupling between charge ordering and phonons, made plausible by the occurrence of dynamic Jahn-Teller effect in manganites, lends a certain flavor to our treatment which is reminiscent of polaron physics. Indeed, we have been able to adapt from the literature expressions for polaron-mediated tunneling rates for light interstitials in solids, as influenced by one- and two-phonon processes.

From the derived expression for the line shape we have estimated line shift and linewidth for explicit comparison with Raman experiment in $Pr_{0.63}Ca_{0.37}MnO_3$. In fact, from the low temperature line shift data we have been able to *determine* the coupling constant of the charge-phonon interaction, which is otherwise a floating parameter of the theory. The same value of the coupling constant has then been employed in analyzing the linewidth data. While the agreement between theory and experiment for line shift is quite satisfactory the same cannot be claimed when it comes to the linewidth, especially at low temperatures. Notwithstanding the fact that the extraction of linewidth is always plagued by bigger uncertainties than that of the line shift, as the entire line shape has to be fitted, the linewidth data nevertheless point to the possibility of the dynamics in manganites being far more complex than just charge (dis)ordering. It seems to us that one has to reckon with combined and concomitant presence of spins, orbital ordering, charge ordering, and phonons. The possibility of the occurrence of orbital waves or orbitons in manganites has already been talked about.[22] What is lacking is a complete many body formalism which brings together magnons, orbitons, and phonons.

Finally, we feel that the theory of charge ordering we have formulated is quite generally applicable. Although the theory is unable to explain all the ingredients of the Raman data in $Pr_{0.63}Ca_{0.37}MnO_3$, it may have better success in other oxide systems, e.g., Fe_3O_4.[6] Work in this direction is in progress and will be reported elsewhere.

ACKNOWLEDGMENTS

We thank R. Gupta, V. Pai, and T.V. Ramakrishnan for fruitful discussions, and Kamal Saha for help in generating

the figures. A.K.S. thanks the Department of Science and Technology for financial assistance. We would also like to record our gratitude to C.N.R. Rao for his continued interest in this work.

APPENDIX A

In this appendix we fill in the mathematical steps which have been omitted in Sec. III B and Sec. III C.

First, note from Eq. (2.8) that the Laplace transform of the correlation function is given by

$$\tilde{C}_q(z)=\sum_{\substack{\mu\nu\\ \mu'\nu'}}\langle\mu|\sigma_x|\mu'\rangle\langle\nu'|\sigma_x|\nu\rangle \times\sum_{m_0m_0'}p_{m_0}(m_0,m_0|(\tilde{\mathcal{U}}(z))_{av}|m_0',m_0'), \tag{A1}$$

where $(\tilde{\mathcal{U}}(z))_{av}$ is defined in Eq. (3.14). It is (the Laplace transform of) the averaged time-development operator, averaged over the phonon states as well as the eigenstates of all other pseudospins barring the central one, in the mean-field sense. The quantity p_{m_0} is the Boltzmann factor corresponding to the quantum number m_0 for the central spin [cf. Eq. (3.17)].

Since $(\tilde{\mathcal{U}}(z))_{av}$ is given by Eqs. (3.9) and (3.10) it is now our task to evaluate the matrix elements of the self-energy. These are given by

$$\tilde{\Sigma}_{m_0,m_0'}(z)=(m_0,m_0|\tilde{\Sigma}(z)|m_0',m_0') =\frac{1}{Z_pZ_s}\sum_{\underline{n}_k\underline{n}_k'}\sum_{ss'}e^{-\beta(E_{\underline{n}_k}+E_s)}\left(m_0\underline{n}_ks,m_0\underline{n}_ks\left|\left(\mathcal{L}_I\frac{1}{z-i(\mathcal{L}_p+\mathcal{L}_s)}\mathcal{L}_I\right)\right|m_0'\underline{n}_k's',m_0'\underline{n}_k's'\right).$$

Rewriting the resolvent back in terms of a time integral, we have

$$\begin{aligned}\tilde{\Sigma}_{m_0,m_0'}(z)&=\frac{1}{Z_pZ_s}\int_0^\infty d\tau e^{-z\tau}\sum_{\underline{n}_k\underline{n}_k'}\sum_{ss'}e^{-\beta(E_{\underline{n}_k}+E_s)}(m_0\underline{n}_ks,m_0\underline{n}_ks|(\mathcal{L}_I[e^{i(\mathcal{L}_p+\mathcal{L}_s)\tau}\mathcal{L}_I])|m_0'\underline{n}_k's',m_0'\underline{n}_ks')\\ &=\frac{1}{Z_pZ_s}\int_0^\infty d\tau e^{-z\tau}\sum_{\underline{n}_k\underline{n}_k'}\sum_{ss'}e^{-\beta(E_{\underline{n}_k}+E_s)}\sum_{m_0''m_0'''}\sum_{\underline{n}_k''\underline{n}_k'''}\sum_{s''s'''}(m_0\underline{n}_ks,m_0\underline{n}_ks|\mathcal{L}_I|m_0''\underline{n}_k''s'',m_0'''\underline{n}_k'''s''')\\ &\quad\times e^{i\tau[(E_{\underline{n}_k''}-E_{\underline{n}_k'''})+(E_{s''}-E_{s'''})]}(m_0''\underline{n}_k''s'',m_0'''\underline{n}_k'''s'''|\mathcal{L}_I|m_0'\underline{n}_k's',m_0'\underline{n}_ks'),\end{aligned} \tag{A2}$$

where we have employed completeness relations and the properties of Liouville operators.[9]

Further, we have for instance,

$$(m_0\underline{n}_ks,m_0\underline{n}_ks|\mathcal{L}_I|m_0''\underline{n}_k''s'',m_0'''\underline{n}_k'''s''')=\langle m_0\underline{n}_ks|\mathcal{H}_I|m_0''\underline{n}_k''s''\rangle\delta_{m_0m_0'''}\delta_{\underline{n}_k\underline{n}_k'''}\delta_{ss'''}-\langle m_0'''\underline{n}_k'''s'''|\mathcal{H}_I|m_0\underline{n}_ks\rangle\delta_{m_0m_0''}\delta_{\underline{n}_k\underline{n}_k''}\delta_{ss''} \tag{A3}$$

Therefore, from Eq. (A2),

$$\begin{aligned}\tilde{\Sigma}_{m_0,m_0'}(z)&=\frac{1}{Z_pZ_s}\int_0^\infty d\tau e^{-z\tau}\sum_{\underline{n}_k\underline{n}_k'}\sum_{ss'}e^{-\beta(E_{\underline{n}_k}+E_s)}\sum_{m_0''m_0'''}\sum_{\underline{n}_k''\underline{n}_k'''}\sum_{s''s'''}e^{i\tau[(E_{\underline{n}_k''}-E_{\underline{n}_k'''})+(E_{s''}-E_{s'''})]}[\langle m_0\underline{n}_ks|\mathcal{H}_I|m_0''\underline{n}_k''s''\rangle\delta_{m_0m_0'''}\delta_{\underline{n}_k\underline{n}_k'''}\delta_{ss'''}\\ &\quad-\langle m_0'''\underline{n}_k'''s'''|\mathcal{H}_I|m_0\underline{n}_ks\rangle\delta_{m_0m_0''}\delta_{\underline{n}_k\underline{n}_k''}\delta_{ss''}][\langle m_0''\underline{n}_k''s''|\mathcal{H}_I|m_0'\underline{n}_k's'\rangle\delta_{m_0'''m_0'}\delta_{\underline{n}_k'''\underline{n}_k'}\delta_{s'''s'}\\ &\quad-\langle m_0'\underline{n}_k's'|\mathcal{H}_I|m_0'''\underline{n}_k'''s'''\rangle\delta_{m_0''m_0'}\delta_{\underline{n}_k''\underline{n}_k'}\delta_{s''s'}]\\ &=\frac{1}{Z_pZ_s}\int_0^\infty d\tau e^{-z\tau}\sum_{\underline{n}_k\underline{n}_k'}\sum_{ss'}e^{-\beta(E_{\underline{n}_k}+E_s)}\Bigg\{\delta_{m_0m_0'}\sum_{m_0''}[\langle m_0\underline{n}_ks|\mathcal{H}_I|m_0''\underline{n}_k's'\rangle\langle m_0''\underline{n}_k's'|\mathcal{H}_I|m_0\underline{n}_ks\rangle-\langle m_0\underline{n}_ks|\mathcal{H}_I|m_0'\underline{n}_k's'\rangle\\ &\quad\times\langle m_0'\underline{n}_k's'|\mathcal{H}_I|m_0\underline{n}_ks\rangle]\Bigg\}(e^{i\tau[(E_{\underline{n}_k'}-E_{\underline{n}_k})+(E_{s'}-E_s)]}+e^{-i\tau[(E_{\underline{n}_k'}-E_{\underline{n}_k})+(E_{s'}-E_s)]}),\end{aligned}$$

having made use of delta functions;

$$=\frac{1}{Z_pZ_s}\int_0^\infty d\tau e^{-z\tau}\sum_{\underline{n}_k\underline{n}_k'}\sum_{ss'} e^{-\beta(E_{\underline{n}_k}+E_s)}\Bigg\{\delta_{m_0m_0'}\sum_{m_0''}[\langle m_0\underline{n}_k s|\mathcal{H}_I|m_0''\underline{n}_k' s'\rangle\langle m_0''\underline{n}_k' s'|\mathcal{H}_I(\tau)|m_0\underline{n}_k s\rangle+\langle m_0\underline{n}_k s|\mathcal{H}_I(\tau)|m_0''\underline{n}_k' s'\rangle$$

$$\times\langle m_0''\underline{n}_k' s'|\mathcal{H}_I|m_0\underline{n}_k s\rangle]-[\langle m_0\underline{n}_k s|\mathcal{H}_I|m_0'\underline{n}_k' s'\rangle\langle m_0'\underline{n}_k' s'|\mathcal{H}_I(\tau)|m_0\underline{n}_k s\rangle+\langle m_0\underline{n}_k s|\mathcal{H}_I(\tau)|m_0\underline{n}_k' s'\rangle\langle m_0'\underline{n}_k' s'|\mathcal{H}_I|m_0\underline{n}_k s\rangle]\Bigg\}, \tag{A4}$$

where we have used the Heisenberg time-evolution operators, as in Eq. (2.9).

To simplify Eq. (A4) further, we consider a typical term, e.g.,

$$\sum_{\underline{n}_k\underline{n}_k'}\sum_{ss'}\sum_{m_0''}\frac{e^{-\beta(E_{\underline{n}_k}+E_S)}}{Z_pZ_s}\langle m_0\underline{n}_k s|\mathcal{H}_I|m_0''\underline{n}_k' s'\rangle\langle m_0''\underline{n}_k' s'|\mathcal{H}_I(\tau)|m_0\underline{n}_k s\rangle$$

$$=t^2\sum_{l,l'}\sum_{\underline{n}_k\underline{n}_k'}\sum_{ss'}\sum_{m_0''}\frac{e^{-\beta(E_{\underline{n}_k}+E_S)}}{Z_pZ_s}[\langle m_0\underline{n}_k s|B_0^-B_l^+s_0^+s_l^-+B_0^+B_l^-s_0^-s_l^+|m_0''\underline{n}_k' s'\rangle\langle m_0''\underline{n}_k' s'|B_0^-(\tau)B_{l'}^+(\tau)s_0^+(\tau)s_{l'}^-(\tau)$$

$$+B_0^+(\tau)B_{l'}^-(\tau)s_0^-(\tau)s_{l'}^+(\tau)|m_0\underline{n}_k s\rangle],$$

having substituted for $\mathcal{H}_I$ from Eq. (3.13),

$$=t^2{\sum_l}'\sum_{m_0''}[\langle m_0|s_0^+|m_0''\rangle\langle m_0''|s_0^-(\tau)|m_0\rangle\langle\langle s_l^-(0)s_l^+(\tau)\rangle\rangle\langle\langle B_0^-(0)B_0^+(\tau)\rangle\rangle\langle\langle B_l^+(0)B_l^-(\tau)\rangle\rangle$$

$$+\langle m_0|s_0^-|m_0''\rangle\langle m_0''|s_0^+(\tau)|m_0\rangle\langle\langle s_l^+(0)s_l^-(\tau)\rangle\rangle\langle\langle B_0^+(0)B_0^-(\tau)\rangle\rangle\langle\langle B_l^-(0)B_l^+(\tau)\rangle\rangle], \tag{A5}$$

where we have utilized the properties of spin-$\frac{1}{2}$ ladder operators, neglected off-site correlation in the mean-field sense, and introduced correlation functions, e.g.,

$$\Phi_l^{-+}(\tau)=\langle\langle s_l^-(0)s_l^+(\tau)\rangle\rangle$$

$$=\sum_{ss'}\frac{e^{-\beta E_s}}{Z_s}\langle s|s_l^-|s'\rangle\langle s'|s_l^+(\tau)|s\rangle, \tag{A6}$$

and

$$\Psi_l^{-+}(\tau)=\langle\langle B_l^-(0)B_l^+(\tau)\rangle\rangle$$

$$=\sum_{\underline{n}_k\underline{n}_k'}\frac{e^{-\beta E_{\underline{n}_k}}}{Z_p}\langle\underline{n}_k|B_l^-(0)|\underline{n}_k'\rangle\langle\underline{n}_k'|B_l^+(\tau)|\underline{n}_k\rangle. \tag{A7}$$

The next term, following the above ''typical term'' in Eq. (A5), is simply the one obtained by interchanging τ with $-\tau$. Since we are interested in the Markovian ($z=0$) limit of the self-energy, the two terms together enable us to write the τ-integral from $-\infty$ to $+\infty$. Combining therefore all the contributions occurring in Eq. (A4), we can write

$$\tilde{\Sigma}_{m_0m_0'}(z=0)=t^2\int_{-\infty}^{\infty}d\tau{\sum_l}'\Bigg\{\Phi_l^{-+}(\tau)\Psi_0^{-+}(\tau)\Psi_l^{+-}(\tau)$$

$$\times\Bigg[\delta_{m_0m_0'}\sum_{m_0''}\langle m_0|s_0^+|m_0''\rangle\langle m_0''|s_0^-(\tau)|m_0\rangle$$

$$-\langle m_0|s_0^+|m_0'\rangle\langle m_0'|s_0^-(\tau)|m_0\rangle\Bigg]$$

$$+\Phi_l^{+-}(\tau)\Psi_0^{+-}(\tau)\Psi_l^{-+}(\tau)$$

$$\times\Bigg[\delta_{m_0m_0'}\sum_{m_0''}\langle m_0|s_0^-|m_0''\rangle\langle m_0''|s_0^+(\tau)|m_0\rangle$$

$$-\langle m_0|s_0^-|m_0'\rangle\langle m_0'|s_0^+(\tau)|m_0\rangle\Bigg]\Bigg\}. \tag{A8}$$

Equation (A8) yields four different terms which can be listed as

$$\tilde{\Sigma}_{++}(z=0)=t^2\int_{-\infty}^{\infty}d\tau{\sum_l}'\langle+|s_0^+|-\rangle\langle-|s_0^-(\tau)|+\rangle$$

$$\times\Phi_l^{-+}(\tau)\Psi_0^{-+}(\tau)\Psi_l^{+-}(\tau), \tag{A9}$$

$$\tilde{\Sigma}_{--}(z=0)=t^2\int_{-\infty}^{\infty}d\tau\sum_l{}'\ \langle -|s_0^+|+\rangle\langle +|s_0^-(\tau)|-\rangle \times\Phi_l^{+-}(\tau)\Psi_0^{+-}(\tau)\Psi_l^{-+}(\tau), \tag{A10}$$

$$\tilde{\Sigma}_{+-}(z=0)=-\tilde{\Sigma}_{++}(z=0),$$

$$\tilde{\Sigma}_{-+}(z=0)=\tilde{\Sigma}_{--}(z=0). \tag{A11}$$

Referring to Eq. (3.22), we may further write

$$\tilde{\Sigma}_{++}(z=0)=\frac{t^2}{e^{\frac{1}{2}\beta J(0)M}+e^{-\frac{1}{2}\beta J(0)M}} \times\int_{-\infty}^{\infty}d\tau e^{-2iJ(0)M\tau}\sum_l{}'\ \Psi_0^{-+}(\tau)\Psi_l^{+-}(\tau), \tag{A12}$$

where we have made use of the fact that if the central spin belongs to sublattice A with magnetization $+M$, the nearest neighbor spin must belong to sublattice B with magnetization $-M$.

Note that the correlation functions Ψ's are given by Eq. (A7) wherein the operators B's are defined in the text [cf. Eq. (2.12)]. We have shown elsewhere[16]

$$\Psi_l^{+-}(\tau)=\Psi_l^{-+}(\tau) =\exp\left\{-\sum_{\underline{k}}\left(\frac{G(\underline{k})}{w_0(\underline{k})}\right)\left[\coth\left(\frac{1}{4}\beta w_0(\underline{k})\right)\times(1-\cos w_0(\underline{k})\tau)+i\sin w_0(\underline{k})\tau\right]\right\}, \tag{A13}$$

independent of l. Introducing then the spectral density of the phonon weight factor as

$$j(w)=2\sum_{\underline{k}}G^2(\underline{k})\,\delta(w-w(\underline{k})), \tag{A14}$$

we have, from Eq. (A12),

$$\tilde{\Sigma}_{++}(z=0)=\eta t^2\int_{-\infty}^{\infty}d\tau\,\frac{e^{-2iJ(0)M\tau}}{e^{\frac{1}{2}\beta J(0)M}+e^{-\frac{1}{2}\beta J(0)M}} \times\exp\left\{-\int_0^{\infty}\frac{j(w)}{w^2}\left[\coth\left(\frac{1}{4}\beta w\right)(1-\cos w\tau)+i\sin w\tau\right]\right\},$$

η being the number of nearest neighbors;

$$=\frac{\eta t^2}{e^{\frac{1}{2}\beta J(0)M}+e^{-\frac{1}{2}\beta J(0)M}}\int_{-\infty}^{\infty}d\tau e^{-2iJ(0)M\tau} \times\exp\left\{-\int_0^{\infty}\frac{j(w)}{w^2}\left[\coth\left(\frac{1}{4}\beta w\right)-\frac{\cos w(\tau-i\beta/4)}{\sinh\left(\frac{1}{4}\beta w\right)}\right]\right\}. \tag{A15}$$

Changing the contour of integration over τ, we obtain the result given in Eq. (3.18). Similar steps yield Eq. (3.19).

APPENDIX B

In this Appendix we sketch a mean field, stochastic model calculation for the line shape.[13,14] The model Hamiltonian is given by [cf. Eq. (3.1)]

$$\tilde{\mathcal{H}}(t)=\tilde{\mathcal{H}}_0+\sum_{j=\pm}V_jf_j(t), \tag{B1}$$

where

$$\tilde{\mathcal{H}}_0=\tfrac{1}{2}w_{\underline{q}}\sigma_z, \tag{B2}$$

$$V_+=\tfrac{1}{2}g_{\underline{q}}\sigma_x, \tag{B3}$$

and

$$V_-=-\tfrac{1}{2}g_{\underline{q}}\sigma_x, \tag{B4}$$

The quantity $f_j(t)$ is a dichotomic Markov (telegraph) process, mimicking the fact that the pseudospin operator $s_i^z(t)$ jumps at random between $\frac{1}{2}$ and $-\frac{1}{2}$, due to spin-lattice relaxations.

As shown in Eq. (13) of Ref. 14 (the Laplace transform of) the averaged time-development operator is given by

$$(\overline{\mathcal{U}(z)})_{av}=\sum_{ab}p_a\left(a\left|\left[(z+\lambda)-i\overline{\mathcal{L}_0}-i\sum_j V_j^{\times}F_j-\lambda\mathcal{J}\right]^{-1}\right|b\right), \tag{B5}$$

where $V_j^{\times}$ denotes the Liouville operator associated with V_j and the stochastic "states" $|a)$ and $|b)$ are associated with the spin states $|m_0m_0)$, $|m_0'm_0')$, etc., introduced in the text. Similarly, the Boltzmann weight p_a has two values p_+ and p_-, given by Eq. (3.23). Finally, the projection operator F_j (F_+ and F_-, in the present case) has been defined in Eq. (8) of Ref. 14.

As shown in Eqs. (19) and (20) of Ref. 14, the special structure for the transition matrix $\mathcal{J}$, given in Eq. (3.25) of the text, allows us to derive:

$$(\overline{\mathcal{U}(z)})_{av}=[(\overline{\mathcal{U}^0(z+\lambda)})^{-1}-\lambda]^{-1}, \tag{B6}$$

where

$$\overline{\mathcal{U}^0(z+\lambda)}=\sum_{j=\pm} p_j[(z+\lambda)-i\overline{\mathcal{L}_0}-iV_j^{\times}]^{-1}. \quad \text{(B7)}$$

As in Ref. 14, we are further interested in the motional narrowing limit in which the term $V_j^{\times}$ can be developed as a perturbation. Thus,

$$\overline{\mathcal{U}^0(z+\lambda)}\simeq \frac{1}{z+\lambda-i\overline{\mathcal{L}_0}}\left[1+i\overline{V}^{\times}\frac{1}{z+\lambda-i\overline{\mathcal{L}_0}} -\sum_j p_j V_j^{\times}\frac{1}{z+\lambda-i\overline{\mathcal{L}_0}}V_j^{\times}\frac{1}{z+\lambda-i\overline{\mathcal{L}_0}}\right], \quad \text{(B8)}$$

where

$$\overline{V}^{\times}=\sum_j p_j V_j^{\times}. \quad \text{(B9)}$$

Hence,

$$(\overline{\mathcal{U}^0(z+\lambda)})^{-1} =(z+\lambda-i\overline{\mathcal{L}_0})-i\overline{V}^{\times} +\sum_j p_j\left(V_j^{\times}\frac{1}{z+\lambda-i\overline{\mathcal{L}_0}}V_j^{\times}-\overline{V}_j^{\times}\frac{1}{z+\lambda-i\overline{\mathcal{L}_0}}\overline{V}^{\times}\right), \quad \text{(B10)}$$

In the present example [cf. Eqs. (B3) and (B4)],

$$\overline{V}^{\times}=\frac{1}{2}(p_+-p_-)g_q\sigma_x^{\times}, \quad \text{(B11)}$$

where

$$(p_+-p_-)=M, \quad \text{(B12)}$$

the order parameter. This then yields Eq. (3.32) of the text if we remember that

$$(p_++p_-)=1. \quad \text{(B13)}$$

*Electronic mail: sdgupta@bose.res.in
†Electronic mail: asood@physics.iisc.ernet.in.
‡Also at Jawaharlal Nehru Centre for Advanced Scientific Research, Jakkur, Bangalore - 560 064.

[1] E.J.W. Verwey, P.W. Haayman, and F.C. Romeijin, J. Chem. Phys. **15**, 181 (1947).
[2] C.H. Chen, S.W. Cheong, and S.A. Cooper, Phys. Rev. Lett. **71**, 2461 (1993).
[3] P.D. Battle, T.C. Gibb, and P. Lightfoot, J. Solid State Chem. **84**, 271 (1990).
[4] J.Q. Li, Y. Matsui, S.K. Park, and Y. Tokura, Phys. Rev. Lett. **79**, 297 (1997).
[5] J.M. Tranquada, B.J. Sterulieb, J.D. Axe, Y. Nakamura, and S. Uchida, Nature (London) **375**, 561 (1995).
[6] Rajeev Gupta, Ph. D. Thesis, Indian Institute of Science, Bangalore (unpublished).
[7] H. Kawano, R. Kajimoto, H. Yoshizawa, Y. Tomioka, H. Kuwahara, and Y. Tokura, Phys. Rev. Lett. **78**, 4253 (1997).
[8] J.D. Lee and B.I. Min, Phys. Rev. B **55**, 12 454 (1997).
[9] See, for instance, S. Dattagupta, *Relaxation Phenomena in Condensed Matter Physics* (Academic, Orlando, 1987).
[10] T. Holstein, Ann. Phys. (N.Y.) **8**, 325 (1959); **8**, 343 (1959); I.J. Lang and Y.A. Firsov, Sov. Phys. JETP **16**, 1301 (1962): Y.A. Firsov, *Polarons* (Nauka, Moscow, 1975).
[11] G.D. Mahan, *Many Particle Physics* (Plenum, New York, 1980).
[12] A. Messiah, *Quantum Mechanics*, Vol. II (North Holland, Amsterdam, 1965).
[13] M.J. Clauser and M. Blume, Phys. Rev. B **3**, 583 (1971).
[14] S. Dattagupta, Phys. Rev. B **16**, 158 (1977).
[15] A. Abragam, *The Theory of Nuclear Magnetism* (Oxford University Press, New York, 1961).
[16] S. Dattagupta and H.R. Schober, Phys. Rev. B **57**, 7606 (1998).
[17] K. Hwang and A. Rys, Proc. R. Soc. London, Ser. A **204**, 406 (1951).
[18] C.P. Flynn and A.M. Stoneham, Phys. Rev. B **1**, 3966 (1970); also Yu Kagan and M.I. Klinger, J. Phys. C **7**, 2791 (1974).
[19] H. Teichler and A. Seeger, Phys. Lett. A **82**, 91 (1981).
[20] Rajeev Gupta, G.V. Pai, A.K. Sood, T.V. Ramakrishnan, and C.N.R. Rao (unpublished).
[21] G.V. Pai and T.V. Ramakrishnan (unpublished).
[22] E. Saitoh, S. Okamoto, K.T. Takahashi, K. Tobe, K. Yamamoto, T. Kumura, S. Ishirhara, S. Maekawa, and Y. Tokura, Nature (London) **410**, 180 (2001); also, P.B. Allen and V. Perebeinos, *ibid.* **410**, 155 (2001).